Spontaneous emission from a quasi-two-dimensional Wigner crystal in a multilayer configuration

Z. Lenac
Department of Physics, University of Rijeka, 51000 Rijeka, Croatia
(Received 20 June 2000; published 14 February 2001)

Spontaneous emission (SE) from electrons forming a quasi-two-dimensional Wigner crystal in a dielectric cavity is discussed for a multilayer configuration. All layers in the system are considered as dielectrics with real dielectric constants. Within such a model, we treat SE completely from the quantum-mechanical (QM) point of view, i.e., we use the quantized electromagnetic field in dielectrics and calculate its interaction with electrons in the Wigner crystal. The full QM approach enables us to go beyond the standard dipole approximation and take into account, e.g., the vibration of electrons around their regular positions inside the crystal and the change of electron positions during the deexcitation process. We analyze only the perpendicular transitions, which involve quantum states determined mainly by the image potential. Since this potential is relatively weak for a typical configuration of a Wigner lattice, the corresponding electromagnetic lifetime τ is estimated to be very large ($\tau \lesssim 10^{-3}$ s). We derive a simple expression for the angular distribution of the SE radiation and analyze its possible deviation from the dipole radiation ($\sin^2\theta$) spectrum. For a typical Wigner crystal formed above a liquid He layer we have found no significant corrections to the spectrum obtained in the dipole approximation. We also consider the case of a Wigner crystal in a (micro)cavity between two metallic plates, discuss the effect of the cavity selection rules on the SE rate, and examine the corresponding discrete SE spectrum.

DOI: 10.1103/PhysRevA.63.033815 PACS number(s): 42.50.Lc, 73.21.−b, 78.90.+t

I. INTRODUCTION

Spontaneous emission (SE), which describes the decay of an excited electronic state due to the electron-photon interaction, is obviously a typical quantum-mechanical (QM) problem. The full QM treatment includes the quantization of an electronic system (e.g., discrete electronic states in molecules or atoms) as well as the quantization of the photon field in the surrounding media. In real systems this may be a very difficult task so that one usually describes the excited molecule by a point dipole and calculates its interaction with the electromagnetic field, determined from the Maxwell equations. Such calculations, performed with the help of the Fermi golden rule, then lead to the SE decay rate in the dipole approximation. Interestingly enough, it follows from the fluctuation-dissipation theorem that the same result can be derived within classical electrodynamics (CE) theory [1].

In this paper we wish to discuss the SE from a Wigner crystal. This crystal is formed by electrons at low electron densities ($n \lesssim 10^{12}$ cm^{-2}) and at very low temperatures ($T \lesssim 2$ K). Theoretically predicted more than 60 years ago by Wigner [2] and experimentally verified more than 20 years ago by Greems and Adams [3], this crystal has not yet been completely investigated, mainly because of experimental difficulties in preparing such a peculiar electronic configuration. In the usual theoretical model, which tries to simulate the experimental setup [3,4], electrons are deposited on a dielectric layer (liquid He) with a metallic substrate. Such electrons are delocalized in the perpendicular direction, thus forming a quasi-two-dimensional (2D) crystal along the dielectric surface. The parallel [5,6] as well as the perpendicular excitations [7,8] of a Wigner crystal have already been investigated and here we wish to analyze the electromagnetic SE decay rate [1,9] from the first excited perpendicular state. Note that the metallic substrate below the crystal acts optically as a mirror, so we shall also discuss the case of a Wigner crystal between two metallic plates that behave as a planar optical cavity [10].

The Wigner crystal is obviously *not* a typical electronic system, so the calculation of the SE spectrum within the point-dipole approximation may be inadequate. This approximation holds when the electron deexcitation is localized within a single molecule, but it becomes questionable in a Wigner crystal in which the mean position of the electron in the perpendicular excited state is significantly different from that in the ground state [8]. In order to take into account delocalization effects, which also include the oscillations of Wigner electrons around their regular lattice positions, we shall extend the QM approach beyond the standard dipole theory. The extension requires the quantization of the electromagnetic field, which could be performed in a standard way only for dielectrics with a real dielectric constant [11]. However, this is a good assumption in our model because the He layer (which supports the Wigner crystal) has no optical transitions within the Wigner SE spectrum. Moreover, it also represents a potential barrier (~ 1 eV) that efficiently prevents Wigner electrons from penetrating the metallic substrate. Besides the photon field, we shall also quantize the lateral vibrations of Wigner electrons and describe them as phonons. This will enable us to discuss a possible temperature dependence of the SE decay rate.

In order to draw some general conclusions regarding the SE spectrum, in this paper we shall first develop a theory essentially appropriate for any electron system confined in a planar multilayer geometry. The specific results for the perpendicular SE decay rate from the quasi-2D Wigner crystal are then obtained with the help of one-particle ''hydrogenic'' wave functions [12]. In that sense, this paper is organized as follows. In Sec. II we define the Hamiltonian of our system and represent it in a quantized form appropriate for the de-

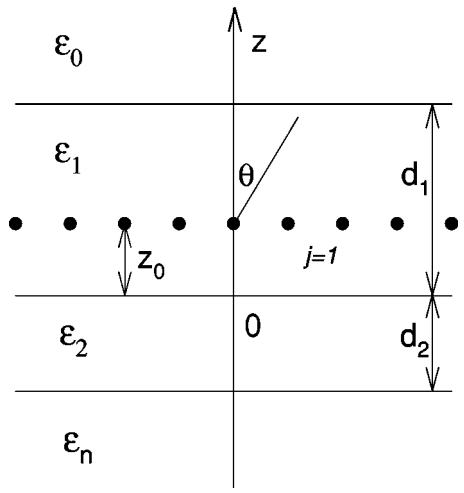

FIG. 1. Geometry of the model. Wigner electrons (black dots) are placed in a dielectric $j=1$.

termination of the SE decay rate. In Sec. III we calculate this rate within both CE and QM theory and, in the latter case, we particularly analyze the extension to the standard dipole approximation. In Sec. IV we give the general results for some typical planar geometries, and in Sec. V we discuss them for two possible configurations of a Wigner lattice. Section VI contains the conclusions.

II. MODEL HAMILTONIAN

We analyze a system of quasi-2D electrons, which form a Wigner crystal. The electrons are well localized in the perpendicular (z) direction and are embedded into a dielectric layer which is surrounded by other planar dielectric layers (Fig. 1). All layers are assumed translationally invariant along the parallel ($\boldsymbol{\rho}$) direction and their dielectric properties are described by a dielectric constant $\epsilon(z)$ which is taken as real.

The electrons of a Wigner crystal interact with a photon field and here we briefly describe the Hamiltonian appropriate for such an interaction. We start by writing the Maxwell equations for the electric field $\mathbf{E}$ and the magnetic induction $\mathbf{B}$ in the medium described by a dielectric constant $\epsilon(\mathbf{r})$

$$\nabla[\epsilon(\mathbf{r})\mathbf{E}(\mathbf{r},t)]=4\pi\rho(\mathbf{r},t),\quad \nabla\times\mathbf{E}(\mathbf{r},t)+\frac{1}{c}\frac{\partial\mathbf{B}(\mathbf{r},t)}{\partial t}=0,$$

$$\nabla\mathbf{B}(\mathbf{r},t)=0,\quad \nabla\times\mathbf{B}(\mathbf{r},t)=\frac{4\pi}{c}\mathbf{j}(\mathbf{r},t)+\frac{1}{c}\frac{\partial[\epsilon(\mathbf{r})\mathbf{E}(\mathbf{r},t)]}{\partial t}. \tag{1}$$

The N electrons of our system, at positions $\mathbf{r}_i$ with mass m, electric charge e, and velocity $\mathbf{v}_i$, form the electric charge density $\rho(\mathbf{r},t)=\Sigma_i e\,\delta(\mathbf{r}-\mathbf{r}_i)$ and the electric current density $\mathbf{j}(\mathbf{r},t)=\Sigma_i e\mathbf{v}_i\delta(\mathbf{r}-\mathbf{r}_i)$, and obey the Lorentz force equation:

$$m\frac{d\mathbf{v}_i}{dt}=e\mathbf{E}_i+\frac{e}{c}\mathbf{v}_i\times\mathbf{B}_i. \tag{2}$$

Here we use the notation $\mathbf{E}_i=\mathbf{E}(\mathbf{r}_i,t),\mathbf{B}_i=\mathbf{B}(\mathbf{r}_i,t)$. We introduce the vector $\mathbf{A}(\mathbf{r},t)$ and the scalar $\Phi(\mathbf{r},t)$ potential in the standard way

$$\mathbf{B}(\mathbf{r},t)=\nabla\times\mathbf{A}(\mathbf{r},t),\quad \mathbf{E}(\mathbf{r},t)=-\nabla\Phi(\mathbf{r},t)-\frac{1}{c}\frac{\partial\mathbf{A}(\mathbf{r},t)}{\partial t}.$$

With the help of the generalized ''transverse gauge''

$$\nabla[\epsilon(\mathbf{r})\mathbf{A}(\mathbf{r},t)]=0, \tag{3}$$

we can derive constitutive equations (1) and (2) from the Lagrangian [11]

$$L=\frac{1}{2}\sum_i mv_i^2+\int\frac{d\mathbf{r}}{8\pi}[\epsilon(\mathbf{r})\mathbf{E}^2-\mathbf{B}^2]$$
$$+\frac{1}{c}\int d\mathbf{r}\mathbf{J}\mathbf{A}-\int d\mathbf{r}\rho\Phi. \tag{4}$$

From Eq. (4) we find the generalized coordinates and the conjugate momenta,

$$\left\{\mathbf{A};\mathbf{P}^A=-\frac{1}{4\pi c}\epsilon\mathbf{E}\right\},\quad \{\Phi;P^\Phi=0\},$$
$$\left\{\mathbf{r}_i;\mathbf{p}_i=m\mathbf{v}_i+\frac{e}{c}\mathbf{A}_i\right\}, \tag{5}$$

which enable us to write the Hamiltonian H of our system in a familiar form,

$$H=H_A+H_e+H_{eA}. \tag{6}$$

Here H_e describes the kinetic energy of electrons in the Wigner crystal together with their Coulomb interaction in the presence of dielectric media,

$$H_e=\sum_i\frac{\mathbf{p}_i^2}{2m}+\frac{1}{2}\sum_i e\Phi_i, \tag{7}$$

H_A represents the photon field energy in a medium with a dielectric constant $\epsilon(\mathbf{r})$,

$$H_A=\int d\mathbf{r}\frac{1}{8\pi}\left[\frac{\epsilon(\mathbf{r})}{c^2}\left(\frac{\partial\mathbf{A}}{\partial t}\right)^2+(\nabla\times\mathbf{A})^2\right], \tag{8}$$

and the interaction between the photon and the crystal field is given by

$$H_{eA}=-\sum_i\frac{1}{2m}\frac{e}{c}[\mathbf{p}_i\mathbf{A}_i+\mathbf{A}_i\mathbf{p}_i]+\sum_i\frac{1}{2m}\frac{e^2}{c^2}\mathbf{A}_i\mathbf{A}_i. \tag{9}$$

In our model, the dielectric constant is not changed inside a dielectric layer. Thus, for all Wigner electrons at $\mathbf{r}_i$ it follows from Eq.(3) that $\nabla_i\mathbf{A}_i=0$, which gives

$$[\mathbf{p}_i,\mathbf{A}_i]=-i\hbar\nabla_i\mathbf{A}_i=0. \tag{10}$$

A. Quantization of the crystal field

The Hamiltonian H_e [Eq. (7)] of the quasi-2D electron system, which polarizes the surrounding dielectric layers, takes the standard form [6]

$$H_e=\sum_i (K_i^{\|}+K_i^{\perp})+\frac{1}{2}\sum_i \sum_{j\neq i} W^{ee}(\boldsymbol{\rho}_{ij},z_i,z_j) + \sum_i W^{im}(z_i), \tag{11}$$

where $K_i^{\|}$ and $K_i^{\perp}$ denote a parallel and a perpendicular kinetic energy of an electron (i), respectively, W^{ee} denotes the interaction between electrons in the presence of a dielectric media at the parallel distance $\boldsymbol{\rho}_{ij}=(\boldsymbol{\rho}_i-\boldsymbol{\rho}_j)$ and at the perpendicular positions (z_i,z_j), and W^{im} describes the interaction of each electron with dielectric layers (image potential).

The assumed localization in the perpendicular direction enables us to factorize the electron wave function Ψ_e into the lateral $v(\boldsymbol{\rho})$ and the perpendicular $u(z)$ component [6],

$$\Psi_e(\boldsymbol{\rho},z)=v(\boldsymbol{\rho})u(z). \tag{12}$$

In the 2D Wigner crystal, the excited perpendicular states correspond to a temperature above 6 K [8], while the crystal exists typically below 2 K. Therefore, we can assume that an electron, possibly excited in the first $(l=1)$ perpendicular state, is surrounded by other electrons in the ground $(l=0)$ perpendicular state. Within the Hartree approximation, we can write

$$u(z)=\prod_{i=1}^{N1} u_0(z_i)\prod_{i=1}^{N2} u_1(z_i), \quad N_1+N_2=N, N_1\gg N_2 \tag{13}$$

where $u_l(z_i)$ are the one-particle variational wave functions.

Let us divide the term W^{ee} (which contains both the parallel and the perpendicular coordinates) into the static W_0^{ee} and the dynamical W_h^{ee} part [6]. The static part describes the average interaction between electrons at their regular lattice sites $\boldsymbol{\rho}_i^0$,

$$W_0^{ee}(z)=\frac{1}{2}\sum_i \sum_{j\neq i} W^{ee}(\boldsymbol{\rho}_{ij}^0,z_i,z_j),$$

and the rest of the W^{ee} interaction is addressed to the dynamical part. This term is obviously not sensitive to the particular wave functions of a few possibly excited electrons, so we can calculate it assuming that all electrons are in their ground perpendicular states,

$$W_h^{ee}(\Delta\boldsymbol{\rho})=\frac{1}{2}\sum_i \sum_{j\neq i} \langle u_0(z_i)u_0(z_j)|[W^{ee}(\boldsymbol{\rho}_{ij},z_i,z_j) - W^{ee}(\boldsymbol{\rho}_{ij}^0,z_i,z_j)]|u_0(z_j)u_0(z_i)\rangle.$$

Now we can divide H_e into the z and $\boldsymbol{\rho}$ dependent part, $H_e=H_e(z)+H_e(\boldsymbol{\rho})$, where

$$H_e(z)=\sum_i [K_i^{\perp}+W^{im}(z_i)]+W_0^{ee}(z) \tag{14}$$

and $H_e(\boldsymbol{\rho})=\Sigma_i K_i^{\|}+W_h^{ee}(\Delta\boldsymbol{\rho})$. Clearly, $u(z)$ and $v(\boldsymbol{\rho})$ in Eq. (12) are now determined as the eigenfunctions of $H_e(z)$ and $H_e(\boldsymbol{\rho})$, respectively. In the harmonic approximation, $H_e(\boldsymbol{\rho})$ describes the phonons of a 2D Wigner crystal [5,6],

$$H_e(\boldsymbol{\rho})=\sum_{\mu}\sum_{\boldsymbol{\kappa}} \hbar\omega_{\mu\boldsymbol{\kappa}}\left(b_{\mu\boldsymbol{\kappa}}^{\dagger}b_{\mu\boldsymbol{\kappa}}+\frac{1}{2}\right), \tag{15}$$

where $b_{\mu\boldsymbol{\kappa}}^{\dagger}(b_{\mu\boldsymbol{\kappa}})$ are standard creation (annihilation) phonon operators of the crystal mode with the polarization $\mu=(L,T)$, the wave vector $\boldsymbol{\kappa}$, and the frequency $\omega_{\mu\boldsymbol{\kappa}}$. Here (L,T) stands for the longitudinal and transverse mode, respectively, and $\boldsymbol{\kappa}$ belongs to the first Brillouin zone.

B. Quantization of the photon field

Let us now quantize the photon field. We must find the eigenmodes $\mathbf{f}_K(\mathbf{r})$ appropriate for our system [11],

$$\nabla\times\nabla\times\mathbf{f}_K(\mathbf{r})=\frac{\epsilon(\mathbf{r})}{c^2}\omega_K^2\mathbf{f}_K(\mathbf{r}), \tag{16}$$

which obey the ''transversality'' conditions

$$\nabla[\epsilon(\mathbf{r})\mathbf{f}_K(\mathbf{r})]=0, \quad \nabla\times\mathbf{f}_K(\mathbf{r})=\text{continuous}. \tag{17}$$

The index K denotes all linearly independent solutions of the eigenequation (16) with eigenfrequencies ω_K. The Hermicity of Eq. (16) leads to the orthonormality condition

$$\int d\mathbf{r}\epsilon(\mathbf{r})\mathbf{f}_K^*(\mathbf{r})\mathbf{f}_{K'}(\mathbf{r})=\delta_{K,K'}. \tag{18}$$

The vector potential is then expanded in terms of the creation $a_K^{\dagger}$ and annihilation a_K operators for photons as

$$\mathbf{A}(\mathbf{r},t)=c\sum_K s_K[a_K(t)\mathbf{f}_K(\mathbf{r})+a_K^{\dagger}(t)\mathbf{f}_K^*(\mathbf{r})]. \tag{19}$$

The quantization requirement

$$[A_{\alpha}(\mathbf{r},t),P_{\beta}^A(\mathbf{r}',t)]=i\hbar\delta_{\alpha,\beta}\delta(\mathbf{r}-\mathbf{r}')$$

leads to the standard commutation relations

$$[a_K(t),a_{K'}^{\dagger}(t)]=\delta_{K,K'}, \quad [a_K(t),a_{K'}(t)]=0,$$

with $s_K=\sqrt{\hbar/\omega_K}$. The Hamiltonian H_A (8) of the photon field now takes the second-quantized form

$$H_A=\sum_K \hbar\omega_K\left(a_K^{\dagger}a_K+\frac{1}{2}\right). \tag{20}$$

III. SPONTANEOUS-EMISSION DECAY RATE

The spontaneous-emission (SE) rate is defined as the inverse lifetime of an excited electronic state which decays

exponentially owing to the interaction with the photon field. As already pointed out, although a typical quantum-mechanical problem, this process can also be treated within the framework of classical electrodynamics. In order to give a clear comparison between the results of the two approaches, we first briefly describe the classical calculation of the SE rate.

A. Classical electrodynamics approach

In classical electrodynamics (CE), an excited molecule with the transition energy $\hbar\omega$ is described by an oscillating point dipole $\mathbf{d}(t)=\mathbf{d}_0\exp(-i\omega t)$ at the molecule position $\mathbf{r}_0$. Then, from Maxwell equations one determines the dipole electric field $\mathbf{E}_d(\mathbf{r},t)=\mathbf{E}_d(\mathbf{r})\exp(-i\omega t)$ and calculates the SE rate as the power lost by the dipole in supporting its own field, normalized to the corresponding photon energy,

$$\gamma^{CE}=\frac{1}{\hbar\omega}\frac{\omega}{2}\mathrm{Im}[\mathbf{E}_d(\mathbf{r}_0)\cdot\mathbf{d}_0^*]. \tag{21}$$

The field of a dipole $\mathbf{E}_d(\mathbf{r})$ in simple layered systems [13] as well as for a general multilayer configuration [14] can be obtained from the corresponding 2D Fourier transform $\mathbf{E}_d(\mathbf{k},z)$ by integration over the parallel wave vector $\mathbf{k}=(k_x,k_y)$. Considering a perpendicular transition ($\mathbf{d}_0=d_0\hat{\mathbf{z}}$), this leads to the following result for the SE rate of the molecule located at z_0 in a jth layer [13,14]:

$$\gamma_j^{CE}=\gamma_{j\infty}^{CE}\Gamma_j^{CE},\quad \gamma_{j\infty}^{CE}=\sqrt{\epsilon_j}\frac{\omega^3}{3\hbar c^3}|\mathbf{d}_0|^2,$$

$$\Gamma_j^{CE}=\frac{3}{2}\mathrm{Re}\int_0^\infty\left(\frac{dkk}{k_j\beta_j}\right)\frac{k^2}{k_j^2}\frac{(1+r_{-j}^p e^{2i\beta_j z_0^-})(1+r_{+j}^p e^{2i\beta_j z_0^+})}{(1-r_{-j}^p r_{+j}^p e^{2i\beta_j d_j})}, \tag{22}$$

where $\gamma_{j\infty}^{CE}$ is the SE rate in the infinite medium (j) with a dielectric constant ϵ_j. Here $k_j=\sqrt{\epsilon_j}\omega/c$ and $\beta_j=\sqrt{k_j^2-k^2}$ are the total and perpendicular photon wave vectors in the jth layer, respectively, d_j is the layer thickness, $z_0^-=z_0$ and $z_0^+=(d_j-z_0)$ are the distances of the dipole from the layer's boundaries, while $r_{-j}^p=r_{j,\ldots,n}^p$ and $r_{+j}^p=r_{j,\ldots,0}^p$ are the standard Fresnel reflection coefficients of the surrounding stacks of layers (see Fig. 1). Note that only p-polarized modes are involved in perpendicular transitions. In the first approximation, we can adopt this simple approach to calculate the SE rate of a weakly excited Wigner crystal by replacing the crystal with a single dipole at the position $\mathbf{r}_0$ where the assumed (local) excitation takes place.

B. Quantum-mechanical approach

To calculate the quantum-mechanical (QM) SE rate, we assume the electron crystal to be initially in the excited state Ψ_e^1 with the energy E_1, and the photon field to be in the vacuum state $|0_f\rangle$. Owing to the interaction with the field, the crystal undergoes the transition to the ground state Ψ_e^0 with the energy E_0, while, simultaneously, a photon K with the energy $\hbar\omega_K$ is created. The Fermi Golden Rule gives for the SE rate,

$$\gamma=\frac{2\pi}{\hbar^2}\sum_K|\langle\Psi_e^1 0_f|H_{eA}|1K\Psi_e^0\rangle|^2\delta(\omega_{10}-\omega_K), \tag{23}$$

where $\hbar\omega_{10}=(E_1-E_0)$ is the excitation energy of the crystal.

We assume that the crystal wave functions are given by Eqs. (12) and (13) and that only one electron is in the first excited perpendicular state $u_1(z_i)$. This gives for the matrix element

$$\langle\Psi_e^1 0_f|H_{eA}|1K\Psi_e^0\rangle=\frac{e}{m}\sqrt{\frac{h}{\omega_K}}T_K,$$

where, from Eqs. (9), (10), and (19), the transition amplitude T_K is given by

$$T_K=\langle v(\boldsymbol{\rho})u_1(z_i)|\mathbf{f}_K(\mathbf{r}_i)\cdot\mathbf{p}_i|u_0(z_i)v(\boldsymbol{\rho})\rangle. \tag{24}$$

Note that in this model the perpendicular transitions are completely decoupled from the parallel electron lattice excitations (phonons), so that in Eq. (24) the same ''parallel'' wave function $v(\boldsymbol{\rho})$ appears in both the Ψ_e^0 and Ψ_e^1 quantum states.

Dipole approximation

In the case of SE from a molecule (or an atom) the position of the transition electron is localized inside a molecule, so that the dipole approximation (DA) usually applies. If the change Δz of the electron position during the transition is much smaller than the wavelength λ of the emitted photon, we can make the same approximation for the Wigner crystal as well. Thus, assuming $\mathbf{r}_0$ as the average electron position, we have $\mathbf{f}_K(\mathbf{r}_i)\simeq\mathbf{f}_K(\mathbf{r}_0)$, so that

$$T_K^{dip}\simeq i\frac{m}{e}\omega_{10}\mathbf{f}_K(\mathbf{r}_0)\cdot\mathbf{d}_{10}^p, \tag{25}$$

where

$$\mathbf{d}_{10}^p=-i\frac{e}{m\omega_{10}}\langle\Psi_e^1|\mathbf{p}_i|\Psi_e^0\rangle \tag{26}$$

is effectively the dipole moment of the crystal. Clearly, if Ψ_e^1 and Ψ_e^0 are the exact eigenfunctions of the Hamiltonian H_e, then, using the identity $\mathbf{p}_i=i(m/\hbar)[H_e,\mathbf{r}_i]$, this dipole moment reduces to the standard transition dipole moment:

$$\mathbf{d}_{10}=e\langle\Psi_e^1|\mathbf{r}_i|\Psi_e^0\rangle. \tag{27}$$

However, since in this work the exact wave functions are not known and $u_l(z)$ are to be determined using the variational method, we retain $\mathbf{d}_{10}^p$ rather than $\mathbf{d}_{10}$ as the relevant transition dipole matrix element.

As in the case of SE from molecules, the SE rate from a Wigner crystal in the dipole approximation is given by the classical result (22), provided that we set $\omega=\omega_{10}$ and let $\mathbf{d}_0\to 2\mathbf{d}_{10}^p$. We can easily check this on the example of SE in

an infinite medium with the dielectric constant $\epsilon=\epsilon_j$. From Eqs. (16) and (18), the appropriate vector-potential eigenfunctions are ($K=\tilde{\mathbf{k}}\nu$)

$$\mathbf{f}_{\tilde{\mathbf{k}}\nu}(\mathbf{r})=\frac{1}{\sqrt{V\epsilon_j}}e^{i\tilde{\mathbf{k}}\cdot\mathbf{r}}\mathbf{e}_{\tilde{\mathbf{k}}\nu},$$

where V is the normalization volume, $\tilde{\mathbf{k}}$ is the three-dimensional photon wave vector, and $\mathbf{e}_{\tilde{\mathbf{k}}\nu}$ are the two orthogonal polarization unit vectors perpendicular to $\tilde{\mathbf{k}}$. With these eigenfunctions in Eq. (25), from Eqs. (23) and (25) we have

$$\gamma_{j\infty}^{dip}=\frac{(2\pi)^2}{\hbar V\epsilon_j}\sum_{\tilde{\mathbf{k}}\nu}\frac{\omega_{10}^2}{\omega_{\tilde{\mathbf{k}}\nu}}|\mathbf{e}_{\tilde{\mathbf{k}}\nu}\cdot\mathbf{d}_{10}^p|^2\delta(\omega_{10}-\omega_{\tilde{\mathbf{k}}\nu}).$$

Converting the sum over $\tilde{\mathbf{k}}$ into the integral in the standard way and using the dispersion relation $\omega_{\tilde{\mathbf{k}}\nu}=\tilde{k}c/\sqrt{\epsilon_j}$ to change to frequency as the integration variable, we find

$$\gamma_{j\infty}^{dip}=\sqrt{\epsilon_j}\frac{4\omega_{10}^3}{3\hbar c^3}|\mathbf{d}_{10}^p|^2, \tag{28}$$

which is the familiar QM result for the SE rate in a lossless medium.

In deriving this result we have neglected the difference between the macroscopic field $\mathbf{E}$ and the local field $\mathbf{E}_{loc}$ actually acting on electrons. In consideration of molecular (atomic) SE, the local field is usually macroscopically calculated assuming a small real [11] or virtual [15] cavity around the excited molecule, whereas most microscopic considerations of a dielectric medium agree with the virtual cavity result for the local field [16–18]. The effect of the local field on the SE rate in a nonabsorbing isotropic medium can then formally be taken into account (in both the CE and QM approaches) by rescaling the corresponding dipole moment: $\mathbf{d}\rightarrow L\mathbf{d}$ [16]. This gives $|L|^2$ as the local-field correction factor to the SE rate, where $L=3\epsilon_j/(2\epsilon_j+1)$ in the real cavity [11] and $L=(\epsilon_j+2)/3$ in the virtual cavity [15–18] model for the local field. It is expected that the same local-field correction factor should apply to the SE rates of molecules in an inhomogeneous system, supposing they are not too close to an interface. As concerns SE from a Wigner crystal, it is natural to consider systems with Wigner electrons immersed in vacuum, as in our calculations performed in Sec. V. These electrons are well separated from the supporting He layer (a dielectric constant which is also close to one), so that we shall neglect local-field effects in further considerations.

Beyond the dipole approximation

Let us now discuss the general case in which the average position of a spontaneously emitting electron differs markedly in the ground and first excited state, so that the dipole approximation could be unsatisfactory.

Owing to the planar geometry of the system we can in general write

$$\mathbf{f}_K(\mathbf{r})=\frac{1}{\sqrt{A}}e^{i\mathbf{k}\cdot\boldsymbol{\rho}}\mathbf{f}_{\mathbf{k}\beta}^{\nu\sigma}(z), \tag{29}$$

where A is the normalization area and the quantum number K comprises the 2D parallel wave vector $\mathbf{k}$, the perpendicular wave vector β in a suitably chosen layer, the polarization index $\nu=(p,s)$ (see Appendix A), and the index σ denoting the type of the mode. We shall be concerned mainly with the *radiation* (propagating) modes with the dispersion relation

$$\omega_K=\omega_{\mathbf{k}\beta}=\frac{c}{\sqrt{\epsilon}}(k^2+\beta^2)^{1/2}, \tag{30}$$

so from now on we shall omit the index σ. The dispersion relation (30) defines the perpendicular wave vector β_l in each dielectric layer l with a dielectric constant ϵ_l: $\beta_l(\omega_K)=[\epsilon_l\omega_K^2/c^2-k^2]^{1/2}$.

Inserting Eq. (29) into Eq. (24) and decompositing the momentum operator according to $\mathbf{p}_i=\mathbf{p}_i^{\perp}+\mathbf{p}_i^{\parallel}$, we have $T_K=T_K^{\perp}+T_K^{\parallel}$, where

$$T_K^{\perp}=\frac{1}{\sqrt{A}}\langle u_1(z_i)|\mathbf{f}_{\mathbf{k}\beta}^{\nu}(z_i)\cdot\mathbf{p}_i^{\perp}|u_0(z_i)\rangle\langle v(\boldsymbol{\rho})|e^{i\mathbf{k}\cdot\boldsymbol{\rho}_i}|v(\boldsymbol{\rho})\rangle,$$

$$T_K^{\parallel}=\frac{1}{\sqrt{A}}\langle u_1(z_i)|\mathbf{f}_{\mathbf{k}\beta}^{\nu}(z_i)|u_0(z_i)\rangle\cdot\langle v(\boldsymbol{\rho})|e^{i\mathbf{k}\cdot\boldsymbol{\rho}_i}\mathbf{p}_i^{\parallel}|v(\boldsymbol{\rho})\rangle.$$

In the dipole approximation ($\mathbf{r}_i\rightarrow\mathbf{r}_0$), the transition amplitude $T_K^{\perp}$ remains finite while both terms in $T_K^{\parallel}$ tend to zero. Therefore, we assume that $T_K^{\perp}$ generally dominates $T_K^{\parallel}$. Introducing the parallel displacements from the equilibrium positions of the lattice electrons $\mathbf{u}_i=(\boldsymbol{\rho}_i-\boldsymbol{\rho}_i^0)$, we obtain

$$T_K\approx T_K^{\perp}=\frac{1}{\sqrt{A}}\langle u_1(z_i)|f_{k\beta}^{p\perp}(z_i)p_i^{\perp}|u_0(z_i)\rangle e^{i\mathbf{k}\cdot\boldsymbol{\rho}_i^0}e^{-(1/2)D(k)}, \tag{31}$$

where

$$D(k)=\langle v(\boldsymbol{\rho})|(\mathbf{k}\cdot\mathbf{u}_i)^2|v(\boldsymbol{\rho})\rangle$$

defines the standard Debye-Waller factor. Here it describes the suppression of the ''perpendicular'' spontaneous emission due to the parallel oscillations of electrons in the Wigner crystal. Using the standard expansion of the electron displacement $\mathbf{u}_i$ in terms of the phonon operators ($b_{\mu\boldsymbol{\kappa}},b_{\mu\boldsymbol{\kappa}}^{\dagger}$), we have [5,19]

$$D(k)=\sum_{\mu}\sum_{\boldsymbol{\kappa}}\left(\frac{\hbar}{2Nm\omega_{\mu\boldsymbol{\kappa}}}\right)k^2|\cos\Phi_{\mu}(\mathbf{k},\boldsymbol{\kappa})|^2(2n_{\mu\boldsymbol{\kappa}}+1), \tag{32}$$

where $\Phi_{\mu}(\mathbf{k},\boldsymbol{\kappa})$ is the angle between the wave vector $\mathbf{k}$ and the polarization vector of the $(\mu,\boldsymbol{\kappa})$ mode, and $n_{\mu\boldsymbol{\kappa}}=[\exp(\hbar\omega_{\mu\boldsymbol{\kappa}}/kT)-1]^{-1}$ gives the average number of excited phonons at temperature T.

Note that, since only the perpendicular component $f^{p\perp}_{k\beta}$ of the eigenfunction $\mathbf{f}^{\nu}_{\mathbf{k}\beta}$ appears in $T^{\perp}_{K}$, only the *p*-polarized photon modes are involved in the SE process in this approximation. The eigenfunctions $f^{p\perp}_{k\beta}(z)$ in a jth layer are of the general form

$$f^{p\perp}_{k\beta}(z)=F^{p}k(f^{p}_{j}e^{-i\beta_j z}+g^{p}_{j}e^{i\beta_j z}), \tag{33}$$

where the normalization factor $F^{p}(k,\beta)$ and the functions $f^{p}_{j}(k,\beta)$ and $g^{p}_{j}(k,\beta)$ are determined from the boundary (17) and normalization (18) conditions (see Appendix A). Since only *p*-polarized modes are relevant, we can use in Eq. (23)

$$\sum_{K}=\sum_{\beta}\sum_{\mathbf{k}}=\sum_{\beta}\frac{A}{(2\pi)^2}\int_0^{2\pi}d\phi\int_0^{\infty}dk\,k.$$

This gives for the QM SE rate of the Wigner crystal located in the jth layer

$$\gamma_j=\gamma^{dip}_{j\infty}\Gamma_j,$$

$$\Gamma_j=\frac{3}{2}\pi\epsilon_j\sum_{\beta}\int_0^{\infty}dk\frac{k^3}{k_j^3}|F^{p}|^2 v_{10}(\beta)e^{-D(k)}\delta(\omega_{10}-\omega_{k\beta}), \tag{34}$$

where $\gamma^{dip}_{j\infty}$ is given by Eq. (28), with the perpendicular dipole moment (26)

$$d^{p}_{10}=-i\frac{e}{m}\frac{1}{\omega_{10}}\langle u_1(z)|p_z|u_0(z)\rangle. \tag{35}$$

We have introduced the dimensionless factor

$$v_{10}(\beta_j)=\left|\frac{\langle u_1(z)|(f^{p}_{j}e^{-i\beta_j z}+g^{p}_{j}e^{i\beta_j z})\dfrac{\partial}{\partial z}|u_0(z)\rangle}{\langle u_1(z)|\dfrac{\partial}{\partial z}|u_0(z)\rangle}\right|^2, \tag{36}$$

which, through the electron wave functions $u_l(z)$, implicitly takes into account the perpendicular delocalization of the electron during the $(1\rightarrow 0)$ transition.

The SE rate in the dipole approximation γ^{dip}_{j} is obtained by letting $z\rightarrow z_0$ and $\boldsymbol{\rho}_i\rightarrow\boldsymbol{\rho}^{0}_{i}$ in Eq. (34). The $z\rightarrow z_0$ limit transforms $v_{10}(\beta_j)$ into

$$v_{z0}(\beta_j)=|f^{p}_{j}e^{-i\beta_j z}+g^{p}_{j}e^{i\beta_j z}|^2, \tag{37}$$

which is independent of the electron wave functions $u_l(z)$. The limit $\boldsymbol{\rho}_i\rightarrow\boldsymbol{\rho}^{0}_{i}$ gives $D(k)\rightarrow 0$, so the influence of the electron delocalization on the SE rate is completely neglected. Notice that in our model one can still allow the dipole at z_0 to oscillate in the parallel direction. In this case $D(k)$ does not vanish, and Eq. (34) describes the SE rate from the strictly 2D Wigner crystal, configured in the plane $z=z_0$.

IV. RESULTS FOR DIFFERENT GEOMETRIES

Further examination of the (normalized) SE rate (34) is possible only for a given geometry, from which one has to determine the plane-wave factors $(F^{p},f^{p}_{j},g^{p}_{j})$. Let us discuss in more detail three simple but qualitatively different cases.

A. Two semi-infinite dielectrics

We assume that two dielectrics, divided by the $z=0$ plane, occupy the whole space $(d_1\rightarrow\infty,d_2\rightarrow\infty)$ and the Wigner crystal lies in the upper layer $(j=1)$ (Fig. 1). The boundary conditions allow two types of modes (Appendix A) that contribute to the SE rate.

1. Type-I modes $[k\leqslant k_1=\sqrt{\epsilon_1}(\omega_{10}/c)]$

Type-I modes are defined for $\beta_1^2>0$, so we shall transform the summation over β values and accordingly the δ function in Eq. (34) as

$$\sum_{\beta}=\sum_{\beta_1}=\frac{L}{2\pi}\int d\beta_1,$$

$$\delta(\omega_{10}-\omega_{\beta_1 k})=\frac{\epsilon_1}{\beta_1}\frac{\omega_{10}}{c^2}\delta(\beta_1-\beta_1(\omega_{10})). \tag{38}$$

With the appropriate plane-wave functions [Eqs. (A4) and (A5)], the contribution from the type-I modes to the normalized SE rate becomes

$$\Gamma^{I}_{1}=\frac{3}{4}\int_0^{k_1}\left(\frac{dkk}{k_1\beta_1}\right)\frac{k^2}{k_1^2}v^{I}_{10}(\beta_1)e^{-D(k)}. \tag{39}$$

2. Type-II modes $[k\leqslant k_2=\sqrt{\epsilon_2}(\omega_{10}/c)]$

Type-II modes are defined for $\beta_2^2>0$. In that case, instead of transformations (38), it is more appropriate to use the transformations

$$\sum_{\beta}=\sum_{\beta_2}=\frac{L}{2\pi}\int d\beta_2,$$

$$\delta(\omega_{10}-\omega_{\beta_2 k})=\frac{\epsilon_2}{\beta_2}\frac{\omega_{10}}{c^2}\delta[\beta_2-\beta_2(\omega_{10})]. \tag{40}$$

The corresponding plane-wave functions [Eqs. (A6) and (A7)] now define the contribution from the type-II modes to the normalized SE rate,

$$\Gamma^{II}_{1}=\frac{3}{4}\int_0^{k_2}\left(\frac{dkk}{k_2\beta_2}\right)\frac{k^2}{k_1k_2}v^{II}_{10}(\beta_1)e^{-D(k)}. \tag{41}$$

The *total* normalized SE rate (34) contains the contribution from both types of modes:

$$\Gamma_1=\Gamma^{I}_{1}+\Gamma^{II}_{1}. \tag{42}$$

The calculation of $v^{I}_{10}(\beta_1)$ or $v^{II}_{10}(\beta_1)$ from Eq. (36) requires the knowledge of perpendicular wave functions. How-

ever, in the dipole approximation (DA), the corresponding matrix elements v_{z0} (37) do not depend upon $u_l(z)$, so we obtain

$$v^I_{z0}(\beta_1)=(1+|r^p_{12}|^2)+2\mathrm{Re}(r^p_{12}e^{2i\beta_1 z_0}),$$

$$v^{II}_{z0}(\beta_1)=(\epsilon_2/\epsilon_1)^2|1-r^p_{12}|^2|e^{2i\beta_1 z_0}|.$$

The corresponding CE result follows from Eq. (22):

$$\Gamma^{CE}_1=\frac{3}{2}\mathrm{Re}\int_0^{k_M}\left(\frac{dkk}{k_1\beta_1}\right)\frac{k^2}{k_1^2}(1+r^p_{12}e^{2i\beta_1 z_0}),$$

where the upper integration limit is $k_M=\max(k_1,k_2)$. This is exactly the same result (42) as derived in the DA, although it is rather difficult to prove it analytically.

If the whole space is occupied by the same dielectric ($\epsilon_2=\epsilon_1$), we obtain the obvious result $\Gamma^{dip}_1=\Gamma^{CE}_1=1$. Notice that the $\epsilon_2\to\epsilon_1$ limit has no physical sense in the QM case if $v_{10}(\beta_1)$ are determined by the wave functions $u_l(z)$, because in our model these wave functions should vanish for $z<0$.

B. Two dielectrics on a metallic plate

We discuss a system in which an infinite dielectric ($d_1\to\infty$) at $z>0$ is separated by a dielectric plate at $-d_2<z<0$ from an infinite metallic substrate at $z<-d_2$ (Fig. 1). A metallic plate is described by an infinite dielectric constant so that the boundary conditions allow only type-I modes (Appendix A). This means that in the calculation of the normalized SE rate (34) we can use the transformations (38).

Let us assume that a Wigner crystal lies in the upper dielectric layer ($j=1$). Inserting the appropriate plane-wave functions [Eqs. (A8) and (A9)] into Eq. (34) we find

$$\Gamma_1=\frac{3}{4}\int_0^{k_1}\left(\frac{dkk}{k_1\beta_1}\right)\frac{k^2}{k_1^2}v_{10}(\beta_1)e^{-D(k)}. \tag{43}$$

In the DA, we obtain

$$v_{z0}(\beta)=2[1+\mathrm{Re}(g^p_1e^{2i\beta_1 z_0})].$$

Exactly the same result follows (even analytically) from Eq. (22) in the corresponding CE approach.

From Eq. (43) one can easily derive the angular distribution of SE radiation. Letting $k=k_1\sin\theta$ we can write the space angle (averaged over the polar angle ϕ) as $d\Omega_1=\sin\theta d\theta=(dkk/k_1\beta_1)$. Therefore the SE radiation emitted in the upper half-space in the θ direction (Fig. 1) is given as

$$\Gamma_1(\theta)\equiv d\Gamma_1/d\Omega_1=\frac{3}{4}\sin^2\theta v_{10}(\beta_1)e^{-D(k)}. \tag{44}$$

Here $\beta_1=k_1\cos\theta$, while β_2 remains real only for $k<k_2$. For $\epsilon_2<\epsilon_1$, it becomes purely imaginary in the region $k_2<k<k_1$ and for those k values the radiation is totally reflected from the dielectric (2).

In the $d_2\to 0$ limit, the present geometry describes a semi-infinite dielectric (with a Wigner crystal) at $z>0$ on a semi-infinite metal at $z<0$, and this limit could not be obtained in the preceding section. In the $d_2\to\infty$ limit, one obtains two semi-infinite dielectric layers. Formally, one can set $\exp(2i\beta_2 d_2)\to 0$, which gives $g^p_1\to r^p_{12}$ and Eq. (43) leads to Eq. (39), i.e., it reproduces the contribution only from type-I modes because it still takes into account the influence of the metallic plate in the infinity which suppresses the type-II modes. To obtain the contributions from both modes as in the preceding section (i.e., without an influence of a metallic plate), one has to be rather careful and make a clear (although inconsistent) replacement: $\exp(2i\beta_2 d_2)\to 0$, $|\exp(2i\beta_2 d_2)|^2\to 1$. This means that, in calculating $v_{10}(\beta_1)$ or $v_{z0}(\beta_1)$ in order to determine the SE rate (43), one has to take $f^p_1=1$, $g^p_1\to r^p_{12}$, $|g^p_1|^2\to 1$.

A qualitatively different situation is obtained if one puts a Wigner crystal in the lower dielectric ($j=2$), i.e., at $-d_2<z<0$. As before, one can take the appropriate plane-wave functions [Eqs. (A8) and (A10) from Appendix A] and insert them into Eq. (34) to calculate the SE rate. However, an obvious problem arises if one tries to use the ''hydrogenic'' wave functions, appropriate for a semi-infinite space, so as to describe a Wigner crystal embedded in a dielectric layer with a finite thickness. This problem will be discussed in more detail in the next section.

C. Two dielectrics between two metallic plates

Here we discuss a model of a ''dielectric cavity,'' in which two dielectric layers are bounded by two semi-infinite metallic plates. The dielectrics with $\epsilon=\epsilon_1$ and $\epsilon=\epsilon_2$ are confined at $0<z<d_1$ and $-d_2<z<0$, respectively, and metallic plates with $\epsilon=\infty$ occupy the rest of the space (Fig. 1). Since there is no electromagnetic field in that space, the boundary conditions allow neither type-I nor type-II modes. Instead, from Appendix A it follows that only discrete values of parameter β are allowed, which we enumerate by index (n):

$$\sum_\beta=\sum_{\beta^{(n)}}=\sum_n, \quad \delta(\omega_{10}-\omega_{\beta_j^{(n)}k})=\frac{\epsilon_j}{k}\frac{\omega_{10}}{c^2}\delta(k-k^{(n)}). \tag{45}$$

The allowed wave vectors are defined for both values ($j=1,2$) in the same way: $k^{(n)}=\sqrt{k_j^2-\beta_j^{(n)2}}$. The solutions exist if either $\beta_1^2\geqslant 0$ or $\beta_2^2\geqslant 0$, i.e., because of the perfect screening of the metallic plates there are no true surface modes with wave vectors that satisfy $\beta_1^2<0, \beta_2^2<0$.

To be specific, let us assume that the crystal lies in the upper dielectric ($j=1$). Using the transformations (45), the normalized SE rate (34) becomes

$$\Gamma_1=\frac{3}{2}\pi\epsilon_1 k_1\sum_n\frac{k^{(n)2}}{k_1^2}|F^p|^2v^{(n)}_{10}e^{-D(k^{(n)})}. \tag{46}$$

Here $v_{10}^{(n)}$ is determined by Eq. (36) with $\beta_1=\beta_1^{(n)}$ and the normalization factor F^p is given in Appendix A with $k=k^{(n)}$.

In the DA, we set $v_{10}^{(n)}\to v_{z0}^{(n)}$, and $v_{z0}^{(n)}=v_{z0}(\beta_1^{(n)})$ is calculated from Eq. (37),

$$v_{z0}^{(n)}=\left|e^{-i\beta_1^{(n)}z_0}+e^{-i\beta_1^{(n)}(2d_1-z_0)}\right|^2.$$

In the CE approach, which should be equivalent to the DA result, one has obvious numerical difficulties in calculating Γ_1^{CE} from Eq. (22). Namely, exactly at $k=k^{(n)}$ the denominator in the integral vanishes. The integral can be calculated by using mathematical expansion methods, which finally lead to Eq. (46) with $v_{10}^{(n)}\to v_{z0}^{(n)}$.

Quantum cavity

The situation becomes much more transparent in the $d_2\to 0$ limit, in which case a single dielectric ($j=1$) is placed between two metallic plates, thus forming a typical quantum cavity. The eigenvalues (A13), $\beta_1^{(n)}=n\pi/d_1, n=0,1,2\ldots$, are obviously chosen to satisfy the boundary conditions for the electromagnetic field, which must vanish at $z=0$ and $z=d_1$. With these $\beta_1^{(n)}$ values, the normalization factor F_0^p takes a particular simple form (A14) and the normalized SE rate (46) becomes

$$\Gamma_1=\frac{3}{4}\left(\frac{\pi}{k_1d_1}\right)\sum_{n=0}^{n_0}\left[1-n^2\left(\frac{\pi}{k_1d_1}\right)^2\right]c_n v_{10}^{(n)}e^{-D(k^{(n)})}, \tag{47}$$

where $c_0=1/2$ ($c_n=1, n=1,2,3,\ldots$) and the highest summation index follows from $\beta_1^{(n)2}>0$: $n_0=[k_1\pi/d_1]$. Particularly, in the DA we find

$$v_{z0}^{(n)}=2\{1+\cos[2n\pi(1-z_0/d_1)]\},$$

which, inserted into Eq. (47) and with $D(k)=0$, leads to the well-known result for the SE rate of a dipole in an ideal quantum cavity with perfect mirrors [10].

V. DISCUSSION

In order to calculate the SE rate from a Wigner crystal using the results derived in the preceding section, we first must determine the appropriate one-electron wave functions $u_l(z)$. Since the image potential $W^{im}(z)$ represents the dominant interaction in the Hamiltonian $H_e(z)$ [Eq. (14)], we take as the variational functions $u_l(z)$ the ''hydrogenic'' wave functions which are the *exact* wave functions for the $1/z$ potential. Taking the origin at the bottom of the (semi–infinite) layer in which the electron crystal resides, we have for $z>0$ [8]

$$u_0(z)=\sqrt{\alpha}\zeta e^{-\zeta/2},\quad u_1(z)=\sqrt{\alpha}B\zeta\left(1-\frac{b}{2}\zeta\right)e^{-\eta\zeta/2}, \tag{48}$$

and $u_l(z)=0$ for $z<0$. Here $\zeta=2\alpha z$ is the normalized perpendicular coordinate. From the orthonormality requirement

$$\int_0^\infty dz u_l^*(z)u_m(z)=\delta_{lm},\quad \{l,m\}=\{1,2\}, \tag{49}$$

we obtain the coefficients

$$b(\eta)=\frac{(\eta+1)}{3},\quad B^2(\eta)=\frac{3\eta^5}{(\eta^2-\eta+1)}.$$

The variational parameters (α,η) are determined by minimizing the energy of the Wigner lattice in the Hartree approximation [6,8].

With the above wave functions we can easily calculate the relevant matrix elements,

$$\langle u_0|z|u_0\rangle=\frac{1}{4\alpha}I_3^D(1),$$

$$\langle u_1|z|u_1\rangle=\frac{B}{4\alpha}\left[I_3^D(\eta)-bI_4^D(\eta)+\frac{b^2}{4}I_5^D(\eta)\right], \tag{50}$$

$$\langle u_1|z|u_0\rangle=\frac{B}{4\alpha}\left[I_3^D(s_0)-\frac{b}{2}I_4^D(s_0)\right],$$

$$\langle u_1|\frac{\partial}{\partial z}|u_0\rangle=\alpha BS^D(s_0), \tag{51}$$

$$\langle u_1|(f_1^pe^{-i\beta_1z}+g_1^pe^{i\beta_1z})\frac{\partial}{\partial z}|u_0\rangle$$
$$=\alpha B[f_1^pS^D(s_+)+g_1^pS^D(s_-)]. \tag{52}$$

Here we have introduced the dimensionless parameter $D=2\alpha d_1$, where d_1 denotes the finite thickness of a dielectric layer (with a Wigner crystal, Fig. 1). Obviously, the use of the wave functions $u_l(z)$ [Eq. (48)] is not appropriate for finite d_1 values because they do not vanish for $z>d_1$. However, if we assume that the Wigner electrons are localized above the $z=0$ plane, in the first approximation we can still use these wave functions if the contribution to the matrix elements, appearing in $v_{10}(\beta_1)$ [Eq. (36)] from the region $z>d_1$, is negligible. This will be the case if d_1 is much larger than the delocalization parameters of $u_l(z)$, that is, if

$$d_1\gtrsim 10/\alpha\ \text{ and }\ d_1\gtrsim 10/\alpha\eta. \tag{53}$$

The other dimensionless parameters in Eqs. (50)–(52) are

$$s_0=\frac{1}{2}(1+\eta),\quad s_\pm=\frac{1}{2}\left(1+\eta\pm i\frac{\beta_1}{\alpha}\right), \tag{54}$$

while $S^D(s)$ denotes the sum of three integrals,

$$S^D(s)=I_1^D(s)-\frac{(1+b)}{2}I_2^D(s)+\frac{b}{4}I_3^D(s),$$

$$I_n^D(s)=\int_0^D dx x^n e^{-sx}. \tag{55}$$

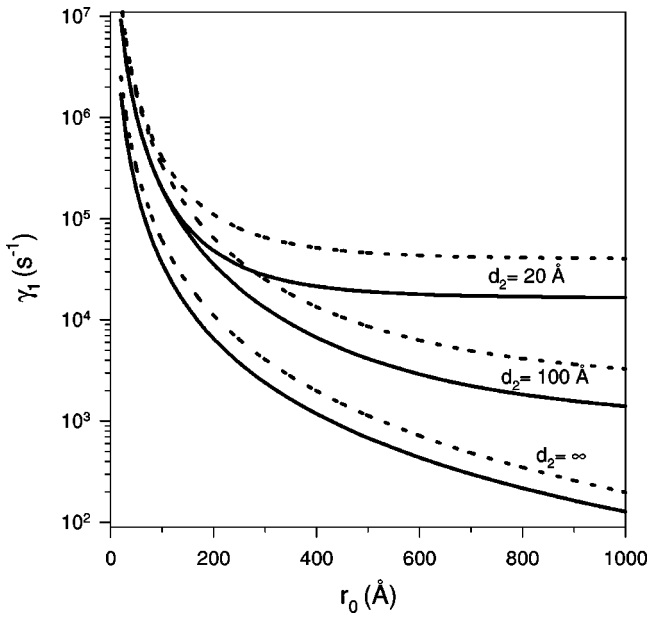

FIG. 2. The SE rate γ_1 as a function of the lattice parameter r_0, shown for different thicknesses d_2 of the He substrate. The dotted lines represent the dipole approximation.

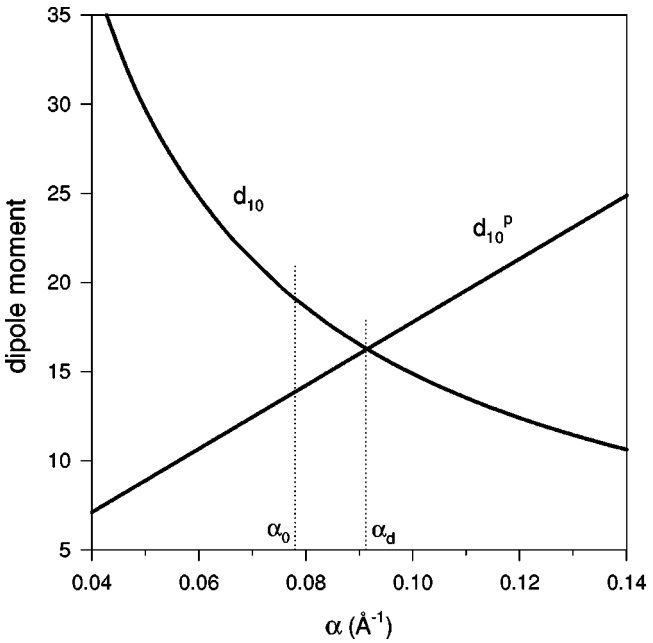

FIG. 3. The transition dipole moments d_{10}^p and d_{10} as functions of a delocalization parameter α. The dipole moments are given in units ea_0 (a_0 is the Bohr radius). The dotted lines denote the ''energy-optimized'' α_0 and the ''dipole-optimized'' α_d values, for $r_0=300$ Å, $d_2=100$ Å.

Note that, in the $d_1\to\infty$ limit, $I_n^D(s)$ simplifies to $I_n^\infty(s)=n!/s^{n+1}$.

We first consider the usual system geometry, here termed *two dielectrics on a metallic plate*, in which the electrons are located above a dielectric layer on a metallic substrate. The SE rate γ_1 for a Wigner crystal in the vacuum ($\epsilon_1=1$) separated by a thin liquid helium ($\epsilon_2=1.0572$) layer from a metallic ($\epsilon_3=\infty$) substrate is shown by full curves in Fig. 2. Obviously, with increasing r_0 or d_2, the interaction between Wigner electrons and their interaction with the image potential becomes weaker. As a consequence, Wigner electrons become more delocalized, which leads to the smaller values of the transition-matrix element and, finally, to the smaller SE rates. For the typical values of a Wigner lattice $r_0=1000$ Å and $d_2=100$ Å, we find $\alpha=0.0417$ Å^{-1}, $\eta=0.765$, and $\omega_{10}=0.0105eV$. This gives a very large electromagnetic lifetime of the first excited perpendicular state, $\tau=1/\gamma_1\approx 0.71\times 10^{-3}$ s, as well as a significant change in the average electron position during the transition [see Eq. (50)]: $\Delta z=\langle u_1|z|u_1\rangle-\langle u_0|z|u_0\rangle\approx 53$ Å. Note, however, that the wavelength of the emitted photon $\lambda=2\pi c/\omega_{10}\approx 1.18\times 10^6$ Å is still much larger than the average electron displacement Δz.

Since $\Delta z/\lambda\ll 1$ for the typical values of r_0 and d_2, the dipole approximation holds perfectly well and one cannot distinguish between γ_1 and γ_1^{dip} in Fig. 2. Ultimately, this is due to the low-electron density in the Wigner crystal leading to a weak electron interaction and, accordingly, to the low transition frequencies. If one increases the electron density, the emitted photon wavelength decreases, but the electron delocalization also decreases simultaneously [6,8]. We find $\alpha\lambda>100$ typically at all electron densities implying $s_\pm\simeq s_0$ in Eq. (52), i.e., the validity of the dipole approximation.

The dotted curves in Fig. 2 represent γ_1^{dip} defined, however, with the (perpendicular) dipole moment

$$d_{10}=e\langle u_1(z)|z|u_0(z)\rangle \tag{56}$$

in place of d_{10}^p (26). As already stressed, d_{10}^p and d_{10} coincide if $u_l(z)$ are the *exact* eigenfunctions of the Hamiltonian $H_e(z)$ [Eq. (14)]. For the *variational* wave functions, however, these two dipole moments differ [see Eq. (51)] and have opposite behavior with respect to the delocalization parameter α, i.e., $d_{10}^p\sim\alpha$ while $d_{10}\sim 1/\alpha$. This is also illustrated in Fig. 3, where we have plotted the dependence of these transition dipole moments on α. As seen in this figure, the crossing point α_d, defined by $d_{10}^p(\alpha_d)=d_{10}(\alpha_d)$, does not necessarily coincide with the optimal variational value α_0. Since the SE rate is proportional to the square of the dipole moment and $[d_{10}^p/d_{10}]^2\sim\alpha^4$, even a small deviation of α_0 from α_d leads to a significant difference between the SE rates γ_1^{dip} for the two definitions of the dipole moment, as can be observed in Fig. 2. The same discrepancy was pointed out in Ref.[20], but here we have given a rigorous explanation.

The *angular distribution* of the (normalized) SE rate as given by Eq. (44) is shown in Fig. (4) for several values of the parameter α. It is determined by the standard dipole radiation factor $\sin^2\theta$ modified by the factor $v_{10}(\beta_1)$ [Eq. (36)], which involves the matrix elements given by Eq. (52). The corrections due to the electron delocalization, which enter explicitly into the terms $s_\pm$ [Eq. (54)], become important for $\beta_1/\alpha\gtrsim 1$, i.e., in the case when the electron delocalization ($\sim 1/\alpha$) becomes comparable with the (perpendicular) wavelength ($\sim 1/\beta_1$) of the emitted photon. We see from the

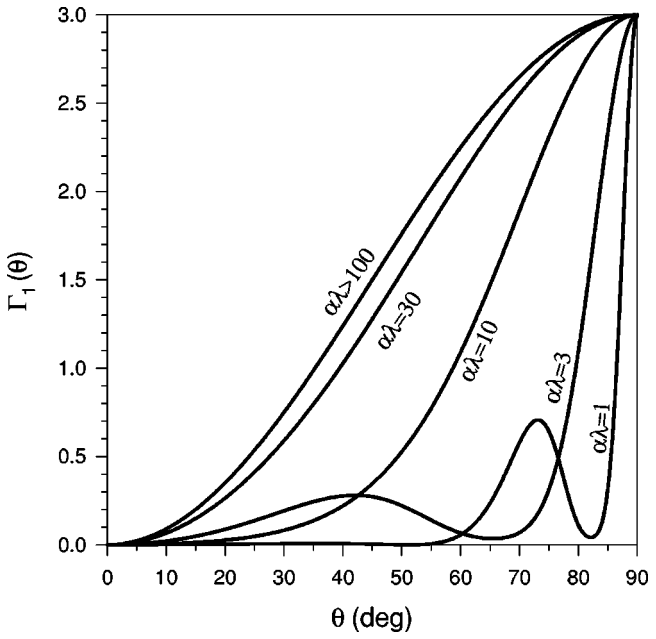

FIG. 4. The angular distribution of the normalized SE rate $\Gamma_1(\theta)$, shown for different delocalization parameters α. The chosen values are $r_0=300$ Å, $d_2=100$ Å, $\lambda=3.9\times10^5$ Å. Note that the influence of a delocalization parameter η (here, $\eta=0.73$) on the SE rate is of much less importance.

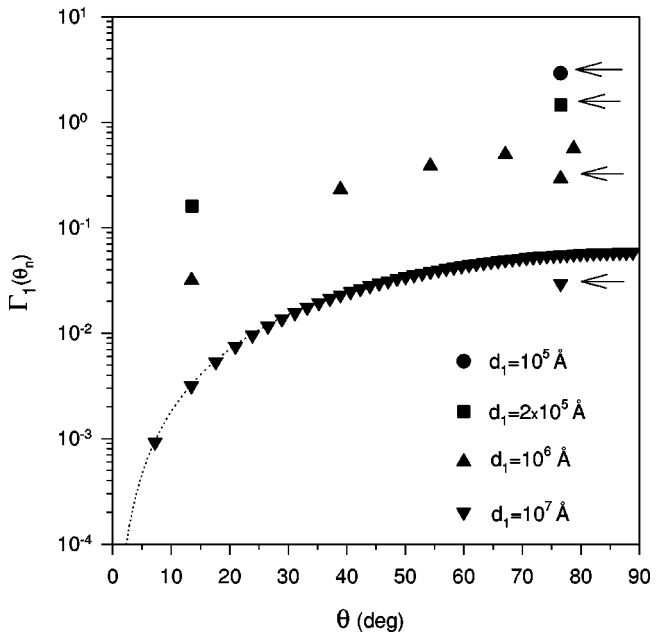

FIG. 5. The angular distribution of the normalized SE rate $\Gamma_1(\theta^{(n)})$. The arrows indicate modes with $\beta_1^2<0$. The dotted line represents the continuum function (44) $\Gamma_1(\theta)$ in arbitrary units.

figure that for $\alpha\gtrsim100/\lambda$ (which is the case of SE from a Wigner crystal), the spectrum approaches that obtained in the dipole approximation ($\alpha\to\infty$), while for lower values of α it markedly differs from the standard $\sin^2\theta$ form and becomes much sharper around the $\theta=90°$ angle.

The *temperature dependence* of the SE rate is given by the Debye-Waller factor $D(k)$. From Eq. (32) follows $D(k)\sim k^2$ and for a reciprocal-lattice vector g_0 one finds $D(g_0)\sim1$ at low temperatures ($T\lesssim2$ K) [5,19] at which the Wigner crystal exists. Since we obtain $k_1/g_0\ll1$ for the highest allowed wave vector ($k=k_1$), we find $D(k)\ll1$ for all $k\leqslant k_1$ wave vectors. This means that we can neglect the influence of parallel oscillations of Wigner electrons, as well as temperature effects, on the perpendicular SE rate.

As a by-product, we can easily calculate the electromagnetic SE rate from *a single electron above a metallic surface* [21]. The electron is trapped by the image potential $W^{im}(z)=-e^2/4z$, so the wave functions $u_l(z)$ are now *exact*. Letting $d_2\to0$ and $r_0\to\infty$, we find $\alpha=1/4a_0, \eta=0.5, \hbar\omega=0.638eV, \lambda=1944$Å$, \Delta z=9.5$Å , so the dipole approximation obviously holds. From Eqs. (35) and (56) we find the dipole moment $d_{10}^p=d_{10}=2.235ea_0$, and the electromagnetic SE rate (34) is $\gamma=2.755\times10^6\ \text{s}^{-1}$.

It is well known that much larger SE rates for an electron above a metallic surface are derived when other decaying mechanisms are taken into account. Besides the electromagnetic coupling, the image states couple with the metallic substrate through the penetration of the image state wave functions $u_l(z)$ into the metal and through the evanescent tails of bulk and surface states outside the metal [21]. However, in the case of a Wigner crystal on a dielectric layer, this layer (liquid He) provides a potential barrier which separates Wigner electrons from electrons in a metallic substrate, so we expect that other mechanisms are not of great importance.

We have also considered the geometry, here termed *two dielectric layers between two metallic plates*, in which the Wigner crystal is embedded at $0<z<d_1$ in the dielectric (vacuum) layer of finite thickness, and the space $z>d_1$ being occupied by another metal (Fig. 1), i.e., effectively in a planar cavity formed by two metallic (perfect) mirrors. The electron localization, besides the image potential, can be also supported by the external pressing field, in which case the metallic plates obviously represent electrodes in the usual experimental configuration [3,4]. As discussed in Ref.[8], the influence of the pressing field on the delocalization parameters α,η is not significant. This means that we can still use the wave functions $u_l(z)$ (48) in the present situation, providing that the electrons are localized above the $z=0$ plane in such a way as to satisfy Eqs. (53).

The normalized rate $\Gamma_1(\theta^{(n)})$ [Eq. (46)] for SE at a discrete angle $\theta^{(n)}=\arcsin(k^{(n)}/k_1)$ is shown in Fig. 5. For the chosen system parameters $d_2=100$ Å and $r_0=300$ Å, we find the delocalization parameters $\alpha=0.0778$ Å^{-1} and $\eta=0.732$. Therefore, our wave functions give correct results for $d_1\gtrsim100$ Å. At the wavelength of the emitted photon $\lambda=3.890\times10^5$ Å ($\omega_{10}=0.03187eV$), according to the dispersion relation (A11), for $d_1=10^5$Å there exists only one mode near $\theta^{(1)}=76.5°$. Owing to SE into only one mode, we obtain an enhanced rate, namely, at such upper layer thicknesses the system acts as a microcavity. We note that for this mode $\beta_1^2<0$ and $\beta_2^2>0$ and, accordingly, it represents a guided mode of the He layer. This mode was nonexistent in the previously considered case $d_1=\infty$ owing to the asymptotic conditions at $z\to\infty$. The number of higher-order, ''ordinary'' ($\beta_1^2>0$ and $\beta_2^2>0$) modes depends on the layer thicknesses and, since $\epsilon_2\simeq\epsilon_1=1$, it can be roughly esti-

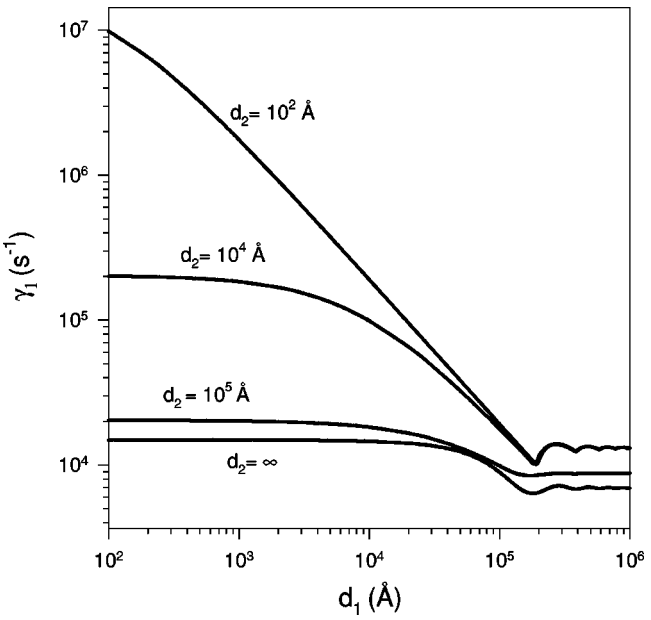

FIG. 6. The SE rate γ_1 as a function of the thickness d_1 of the vacuum layer, shown for different thicknesses d_2 of the He substrate. Note that both axes are given in a logarithmic scale.

mated from the mode condition for a planar cavity [Eq. (A13) with $d_1 \rightarrow (d_1+d_2)$],

$$\cos(\theta^{(n)}) \simeq \frac{n}{2}\frac{\lambda}{(d_1+d_2)},$$

where n is an integer. This gives the critical value $d_1^c \approx \lambda/2 = 1.945\times 10^5$ Å for the appearance of the next mode, which is practically the exact result. Accordingly, for $d_1 = 2.0 \times 10^5$ Å, in Fig. 5 we have SE into two modes with the smaller rates. With increasing d_1, the number of modes rapidly increases and at $d_1 = 10^7$ Å the normalized SE rate $\Gamma_1(\theta^{(n)})$ becomes almost a continuous function.

The total SE rate γ_1 [Eq. (34)], summed over all modes, is shown in Fig. 6 as a function of dielectric layer thicknesses. In the region $(d_1, d_2) \lesssim 10^5$ Å the only allowed mode is the above-mentioned guided mode and the relatively large γ_1 is due to the SE into this mode. Owing to the gradual disappearance of this mode with increasing d_1, the SE rate decreases significantly up to the upper layer thickness $d_1 \approx 10^5$ Å. With further increase of d_1, SE into the second- and higher-order (ordinary) modes becomes allowed and γ_1 saturates to a value close to its asymptotic ($d_1 \rightarrow \infty$) limit. For $d_2 > 10^5$ Å, SE into higher-order modes is possible even for small d_1 values and the total SE rate becomes close to its ''continuum'' ($d_2 \rightarrow \infty$) limit, which is not very sensitive to the particular d_1 value.

VI. CONCLUSION

We have analyzed the SE spectrum from a quasi-2D Wigner crystal in order to give more detailed insight into this intriguing system as well as to suggest a possible spectroscopic tool for the Wigner crystal detection. Knowing that a Wigner electron could significantly change its positions during the deexcitation process, we have treated this problem very carefully. The calculations of the SE spectrum are performed within (i) the CE theory, (ii) standard dipole approximation (DA), and (iii) QM theory beyond the DA. The first two approaches, although from quite different points of view, lead to the same result. The corresponding SE spectrum, normalized to the SE rate in an infinite medium, shows an angular distribution typical of the point dipole, and this distribution is not influenced by the shape of the wave functions of the deexcited electron. However, these wave functions explicitly enter into the definition of the SE spectrum in the third approach. Particularly, in the case when the perpendicular delocalization Δz of the deexcited electron is comparable with the emitted photon wavelength λ, we have found a much narrower angular distribution than in the DA. However, for a Wigner crystal, we have typically obtained $\lambda \gg \Delta z$, so the angular distribution remains close to the DA result.

The calculations of the total SE rates (in the DA and above the DA) can lead to different values as a consequence of the different definitions of the transition dipole moments, i.e., d_{10}^p [Eq. (35)] and d_{10} [Eq. (56)]. While those two dipole moments would take the same value for the *exact* electron wave functions, they are usually not known and here we have used the standard variational wave functions $u_l(z)$ [Eq. (48)], optimized to give the best possible energies of the perpendicular Wigner states. We have demonstrated how the electron delocalization, defined by those wave functions, can lead to different values for d_{10}^p and d_{10} and therefore to different values for the corresponding total SE rates γ. However, the normalized SE rates Γ do not depend upon the dipole moment, so the quantitative difference between them has no physical consequences on the understanding of the SE spectrum of the Wigner crystal. In fact, it can eventually serve as a warning for calculations of the total SE rate in similar systems.

We have also analyzed the influence of the lateral delocalization of Wigner electrons on the (perpendicular) SE rate. The lateral electron oscillations have been described in the harmonic approximation as phonons, and the contribution to the SE spectrum has been given by the Debye-Waller factor. It turns out that at low temperatures, at which the Wigner lattice can exist only, the Debye-Waller factor has almost no influence on the perpendicular SE rate. In this sense, the possible corrections to the harmonic approximation [22] or the effects of the electron-ripplon coupling [19] are obviously not important.

We have found that the typical values of the SE rate give long electromagnetic lifetimes ($\lesssim 10^{-3}$ s) of the first excited perpendicular state of the Wigner crystal. This is due to the weak coupling of Wigner electrons to the surrounding media and, accordingly, relatively small transition frequencies. Owing to the corresponding large photon wavelengths, possible nondipole behavior of the SE spectrum does not show up. We have also discussed characteristic properties of the SE spectrum from a Wigner crystal in a microcavity formed by two metallic plates. Such a configuration is experimentally realized, e.g., when using an electric field to additionally

press Wigner electrons towards a liquid-He layer on one of the plates. In this case, Wigner electrons interact with a small number of the cavity modes, and spontaneously emitted photons can therefore be detected only at discrete angles $\theta^{(n)}$ determined by the cavity selection rules, i.e., one has to match the effective cavity thickness $d\cos\theta^{(n)}$ with the wavelength of the SE photons. For a typical density of a Wigner crystal ($r_0 \sim 10^3$ Å) this ''microcavity'' SE spectrum is observed up to $d \lesssim 10^6$ Å as even at these cavity thicknesses the angles $\theta^{(n)}$ remain clearly separated. Since the perpendicular excitation energies of a 2D electron gas and a 2D electron crystal are significantly different for electron densities $n \gtrsim 10^8$ cm^{-2} ($r_0 \lesssim 10^4$ Å) [8], the corresponding emission channels for the SE radiation $\theta^{(n)}$ are also different. Therefore the determination of the allowed channels at a chosen electron density could serve as an optical detector for the existence of the Wigner crystal.

ACKNOWLEDGMENT

The author is grateful to M.S. Tomaš for a number of useful discussions.

APPENDIX A: EIGENFUNCTIONS FOR A MULTILAYER

The eigenfunctions $\mathbf{f}_K(\mathbf{r})$ of a photon field are defined by Eqs. (16)–(18). In the case of a multilayer with a translation invariance along the parallel direction, one has to determine only the z-dependent function $\mathbf{f}_{\mathbf{k}\beta}(z)$ (29). Here $\mathbf{k}$ is a two-dimensional (parallel) wave vector, which together with a (perpendicular) wave vector β, satisfies the wave equation (30): $\beta^2+k^2=\omega_K^2 c^2/\epsilon$, inside a dielectric layer with a dielectric constant ϵ.

The eigenfunction $\mathbf{f}_{\mathbf{k}\beta}(z)$ can be naturally divided into the perpendicular ($\perp$) and parallel ($\parallel$) components: $\mathbf{f}_{\mathbf{k}\beta}(z) = f^{p\perp}_{k\beta}(z)\hat{\mathbf{z}} + f^{p\parallel}_{k\beta}(z)\hat{\mathbf{k}} + f^{s\parallel}_{k\beta}(z)\hat{\mathbf{n}}$. It contains two polarizations: the $\nu=p$ polarization with the component into the $(\hat{\mathbf{k}},\hat{\mathbf{z}})$ plane and the $\nu=s$ polarization with the component in the $\hat{\mathbf{n}}=\hat{\mathbf{k}}\times\hat{\mathbf{z}}$ direction.

Inside a dielectric layer, Eqs. (16), (17), and (29) lead to $(\partial/\partial z) f^{p\perp}_{k\beta}(z) + ik f^{p\parallel}_{k\beta}(z) = 0$ and $(\beta^2+\partial^2/\partial z^2)\mathbf{f}_{\mathbf{k}\beta}(z)=0$, so $\mathbf{f}_{\mathbf{k}\beta}(z)=\mathbf{f}^p_{\mathbf{k}\beta}(z)+\mathbf{f}^s_{\mathbf{k}\beta}(z)$ takes a simple form for both polarizations,

$$\mathbf{f}^p_{\mathbf{k}\beta}(z) = F^p[(\beta\hat{\mathbf{k}}+k\hat{\mathbf{z}})f^p(k)e^{-i\beta z} + (-\beta\hat{\mathbf{k}}+k\hat{\mathbf{z}})g^p(k)e^{i\beta z}], \tag{A1}$$

$$\mathbf{f}^s_{\mathbf{k}\beta}(z) = F^s(\hat{\mathbf{n}})[f^s(k)e^{-i\beta z} + g^s(k)e^{i\beta z}].$$

The boundary conditions (17) require the continuity of

$$\epsilon(f^p e^{-i\beta z} + g^p e^{i\beta z}), \quad \beta(f^p e^{-i\beta z} - g^p e^{i\beta z}),$$

$$\beta(f^s e^{-i\beta z} \pm g^s e^{i\beta z}) \tag{A2}$$

along the perpendicular direction, while the orthonormality equation (18), together with Eq. (29), requires for each polarization

$$\int_{-\infty}^{+\infty} dz\,\epsilon(z)\mathbf{f}^{\nu *}_{\mathbf{k}\beta}(z)\mathbf{f}^{\nu}_{\mathbf{k}\beta'}(z) = \delta_{\beta,\beta'} = \frac{2\pi}{L}\delta(\beta-\beta'). \tag{A3}$$

The last relation holds only for a continuous parameter β, with L as a normalization length. Notice that the parameter β can be either real or imaginary, and we should always require $\mathrm{Re}\,\beta \geqslant 0$, $\mathrm{Im}\,\beta \geqslant 0$.

From Eqs. (A2) and (A3) one can easily determine the coefficients F^ν, g^ν_j, f^ν_j for each medium (j) in a multilayer. The corresponding Fresnel reflectivities between the two dielectric plates (i,j) are defined as [13,14]

$$r^p_{ij} = \frac{\beta_i\epsilon_j - \epsilon_i\beta_j}{\beta_i\epsilon_j + \epsilon_i\beta_j}, \quad r^s_{ij} = \frac{\beta_i - \beta_j}{\beta_i + \beta_j}.$$

Here we need the coefficients only for p-polarized modes.

1. Two semi-infinite dielectrics

Two semi-infinite dielectrics with $\epsilon=\epsilon_1$ and $\epsilon=\epsilon_2$ occupy an upper and a lower half-space, respectively (Fig. 1). From Eqs. (A2) and (A3) we find two types of modes: type-I modes with the incoming wave $\exp(-i\beta_1 z)$ from the upper half-space and type-II modes with the incoming wave $\exp(i\beta_2 z)$ from the lower half-space.

Type-I modes ($\beta_1^2 > 0$):

$$|F^p|^2 = \frac{1}{k_1^2}\frac{1}{\epsilon_1 L}, \quad k_1 = \sqrt{\epsilon_1}\,\frac{\omega_K}{c}, \tag{A4}$$

$$j=1 (z>0): \quad f^p_1 = 1, \quad g^p_1 = r^p_{12}, \tag{A5}$$

$$j=2 (z<0): \quad f^p_2 = (\epsilon_1/\epsilon_2)(1+r^p_{12}), \quad g^p_2 = 0.$$

Type-II modes ($\beta_2^2 > 0$):

$$|F^p|^2 = \frac{1}{k_2^2}\frac{1}{\epsilon_2 L}, \quad k_2 = \sqrt{\epsilon_2}\,\frac{\omega_K}{c}, \tag{A6}$$

$$j=1 (z>0): \quad f^p_1 = 0, \quad g^p_1 = (\epsilon_2/\epsilon_1)(1+r^p_{21}), \tag{A7}$$

$$j=2 (z<0): \quad f^p_2 = r^p_{21}, \quad g^p_2 = 1.$$

2. Two dielectrics on a metallic plate

A semi-infinite dielectric with $\epsilon=\epsilon_1$ lies above a d_2-thick dielectric layer with $\epsilon=\epsilon_2$, which is supported by a semi-infinite metallic plate with $\epsilon=\infty$ (Fig. 1). Only type-I modes are possible because the incoming wave solution exists only for the upper half-space.

Type-I modes ($\beta_1^2 > 0$):

$$|F^p|^2 = \frac{1}{k_1^2}\frac{1}{\epsilon_1 L}, \tag{A8}$$

$$j=1 (z>0): \quad f^p_1 = 1, \quad g^p_1 = \left(\frac{r^p_{12} + \exp(2i\beta_2 d_2)}{1 + r^p_{12}\exp(2i\beta_2 d_2)}\right), \tag{A9}$$

$$j=2(-d_2<z<0): \quad f_2^p=\frac{\epsilon_1}{\epsilon_2}\left(\frac{1+r_{12}^p}{1+r_{12}^p\exp(2i\beta_2 d_2)}\right),$$

$$g_2^p=\exp(2i\beta_2 d_2)f_2^p. \tag{A10}$$

3. Two dielectrics between two metallic plates

A d_1-thick dielectric layer with $\epsilon=\epsilon_1$ lies above a d_2-thick dielectric layer with $\epsilon=\epsilon_2$. Both dielectrics are bounded by two semi-infinite metallic plates with $\epsilon=\infty$, so there are no solutions with incoming waves from either an upper or a lower half-space (Fig. 1). Therefore, we obtain the same form for the coefficients f_j^p, g_j^p as in the case of two dielectrics on a semi-infinite plate [Eqs. (A9) and (A10)], but the additional boundary condition at $z=d_1$ now requires

$$g_1^p(1,2)\equiv\left(\frac{r_{12}^p+\exp(2i\beta_2 d_2)}{1+r_{12}^p\exp(2i\beta_2 d_2)}\right)=e^{-2i\beta_1 d_1}. \tag{A11}$$

This equation has solutions only for discrete $\beta_j^{(n)}$ values ($n=0,1,2,\ldots$). We distinguish the following three cases.

(i) $\beta_1^2\geqslant 0$: In this case we find $|g_1^p(1,2)|=1$ for any β_2, so we can set $g_1^p(1,2)\exp(2i\beta_1 d_1)=\exp[i\Phi(\beta)]$ and the solution of Eq. (A11) is given implicitly as $\Phi(\beta^{(n)})=2\pi n, \quad n=0,1,2,\ldots$.

(ii) $\beta_1^2<0, \beta_2^2\geqslant 0$: In this case we can transform Eq. (A11) into $g_1^p(2,1)=e^{-2i\beta_2 d_2}$. Now we obtain $|g_1^p(2,1)|=1$ for any β_1, so we can find the solutions for $\beta^{(n)}$ in the same way as in i).

(iii) $\beta_1^2<0, \beta_2^2<0$: In this case we find $|g_1^p|<1$, $|\exp(-2i\beta_j d_j)|>1$, so Eq. (A11) has no solution.

Yet, we have to determine the normalization constant F^p. From Eq. (A3) it follows

$$|F^p|^2=[\epsilon_1 e^{2\mathrm{Im}\beta_1 d_1}h^p(\beta_1)+|f_2^p|^2\epsilon_2 e^{-2\mathrm{Im}\beta_2 d_2}h^p(\beta_2)]^{-1}, \tag{A12}$$

$$h^p(\beta_j)=(|\beta_j|^2+k^2)\frac{\sinh(2\,\mathrm{Im}\,\beta_j d_j)}{\mathrm{Im}\,\beta_j}-(|\beta_j|^2-k^2)\frac{\sin(2\,\mathrm{Re}\,\beta_j d_j)}{\mathrm{Re}\,\beta_j}.$$

A particularly simple result follows if only one dielectric, e.g., the dielectric $j=1$, is present. Letting $d_2=0$, we obtain $g_1^p=1$ and the solutions of Eq. (A11) are [9]

$$\Phi(\beta^{(n)})=2\beta_1^{(n)}d_1=2\pi n, \quad n=0,1,2,\ldots,[k_1\pi/d_1] \tag{A13}$$

with the normalization coefficient

$$|F^p|^2=\frac{1}{2\epsilon_1 k_1^2 d_1}\left\{\frac{1}{2},n=0;\,1,n>0\right\}. \tag{A14}$$

[1] L. D. Landau and E. M. Lifshitz, *Statistical Physics* (Pergamon, Oxford, 1980), Chap. 8; G. S. Agarwal, Phys. Rev. A **11**, 230 (1975); **12**, 1475 (1975); J. M. Wylie and J. E. Sipe, *ibid.* **30**, 1185 (1984); **32**, 2030 (1985).

[2] E. P. Wigner, Phys. Rev. **46**, 1002 (1934).

[3] C. C. Grimes and G. Adams, Phys. Rev. Lett. **42**, 795 (1979).

[4] F. I. B. Williams, Surf. Sci. **113**, 371 (1982); R. Mehrotra, C. J. Guo, Y. Z. Ruan, D. B. Mast, and A. J. Dahm, Phys. Rev. B **29**, 5239 (1984); D. C. Glattli, E. Y. Andrei, and F. I. B. Williams, Surf. Sci. **196**, 17 (1988).

[5] R. S. Crandall, Phys. Rev. A **8**, 2136 (1973); L. Bonsall and A. A. Maradudin, Phys. Rev. B **15**, 1959 (1977); F. M. Peeters, *ibid.* **30**, 159 (1984).

[6] Z. Lenac and M. Šunjić, Phys. Rev. B **43**, 6049 (1991); **44**, 11 465 (1991); **46**, 7821 (1992).

[7] C. C. Grimes, T. R. Brown, M. L. Burns, and C. L. Zipfeld, Phys. Rev. B **13**, 140 (1976).

[8] Z. Lenac and M. Šunjić, Phys. Rev. B **48**, 14 496 (1993).

[9] G. Barton, Proc. R. Soc. London, Ser. A **320**, 251 (1970); F. De Martini, M. Marrocco, P. Mataloni, L. Crescentini, and R. Loudon, Phys. Rev. A **43**, 2480 (1991).

[10] P. W. Milonni and P. L. Knight, Opt. Commun. **9**, 119 (1973); H. Rigneault and S. Monneret, Phys. Rev. A **54**, 2356 (1996).

[11] R. J. Glauber and M. Lewenstein, Phys. Rev. A **43**, 467 (1991).

[12] N. M. Fujiki and D. J. W. Geldart, Phys. Rev. B **46**, 9634 (1992).

[13] G. W. Ford and W. H. Weber, Phys. Rep. **113**, 195 (1984).

[14] M. S. Tomaš, Phys. Rev. A **51**, 2545 (1995).

[15] S. M. Barnett, B. Huttner, and R. Loudon, Phys. Rev. Lett. **68**, 3698 (1992); S. M. Barnett, B. Huttner, R. Loudon, and R. Matloob, J. Phys. B **29**, 3763 (1996).

[16] J. Knoester and S. Mukamel, Phys. Rev. A **40**, 7065 (1989).

[17] S. T. Ho and P. Kumar, J. Opt. Soc. Am. B **10**, 1620 (1993).

[18] G. Juzeliunas, Chem. Phys. **198**, 145 (1995); Phys. Rev. A **55**, R4015 (1997).

[19] D.S. Fisher, B. I. Halperin, and P. M. Platzman, Phys. Rev. Lett. **42**, 798 (1979); D. Marty and J. Poitrenaud, J. Phys. (Paris) **45**, 1243 (1984).

[20] Z. Lenac and M. S. Tomaš, Surf. Sci. **454–456**, 1085 (2000).

[21] P. M. Echenique, J. M. Pitarke, E. V. Chulkov, and A. Rubio, Chem. Phys. **251**, 1 (2000).

[22] V. Tozzini and M. P. Tosi, J. Phys.: Condens. Matter **8**, 8121 (1996).